J. Chem. Sci. (2021) 133:52
https://doi.org/10.1007/s12039-021-01911-8

REGULAR ARTICLE

The electrosorption of 3-bromo-2-nitrothiophene on gold as studied with surface-enhanced Raman spectroscopy

ABDEL AZIZ QASEM JBARAH
Department of Chemistry, Faculty of Science, Al-Hussein Bin Talal University, P.O. Box 20, Ma'an, Jordan
E-mail: aajbarah@ahu.edu.jo

MS received 24 July 2020; revised 27 February 2021; accepted 31 March 2021

Abstract. The electrosorption of 3-bromo-2-nitrothiophene on a polycrystalline gold electrode has been studied with surface-enhanced Raman spectroscopy SERS. Results imply a tilted orientation of the 3-bromo-2-nitrothiophene molecule with a sulfur atom of the thiophene ring and oxygen atoms of the nitro group interacting directly with the gold surface. The UV-Vis spectrum of the 3-bromo-2-nitrothiophene is recorded and its results indicated that the SERS spectra were measured under off-resonance conditions. Cyclic voltammetry measurements of the 3-bromo-2-nitrothiophene were made and the oxidation and reduction potentials of the 3-bromo-2-nitrothiophene at the gold electrode have been reported. The experimental infrared and Raman data are supported by density functional theory (DFT) calculations of 3-bromo-2-nitrothiophene using the B3LYP level of theory and 6-31G (d) basis set. The vibrational frequencies of the molecule were computed using the optimized geometry obtained from the DFT calculations. The calculated spectra are very close to the recorded infrared and Raman of the solid 3-bromo-2-nitrothiophene. No imaginary frequencies are observed in the calculated spectra. Also, DFT calculations are performed to predict and investigate the adsorption behavior of 3-bromo-2-nitrothiophene on the Au surface. In this DFT calculations, the adsorbed 3-bromo-2-nitrothiophene on the gold electrode surfaces was modeled as the metal−molecule complex.

Keywords. spectroelectrochemistry; 3-bromo-2-nitrothiophene; electrosorption; Raman; DFT.

1. Introduction

Recently, many experimental works, which are used the surface-enhanced Raman spectra (SERS) technique, have been reported for the adsorbed molecules on silver, gold, and copper surfaces.[1–4] SERS is an important spectroscopic technique that has played an important role in the study of molecules adsorbed on metal surfaces. Also, it has been proven to be a very sensitive method to detect the orientations of the adsorbed molecules with very low concentration levels (ca. 10^{-12} mol dm^{-3}) on Nobel metals. Besides, SERS have also been used as a powerful tool for studying the vibrational spectra of monolayers on silver and gold.[5] Interaction of molecule with certain metal surfaces is an essential point for obtaining surface-enhanced Raman spectra. In general, the molecules show SERS phenomena, governed by physical or chemical adsorption, when it has atoms like sulfur, nitrogen, and oxygen or some functional groups such as CN, SO_3, SH, and COOH which can interact with silver, gold, or copper metal surfaces.[6,7] Several previous studies have used SERS to investigate the surface orientation of the adsorbates having one or more σ donor atoms (N or O) along with π donor system.[8,9] It was reported that the perfect model system for the study of SERS is the pyridine molecule.[10] This is because pyridine has suitable surface coordination property and different bonding modes involving the aromatic π electrons and lone pair electrons of the nitrogen atom. Thiophene and substituted thiophenes have also attracted considerable SERS studies in recent years. Oligomerization of thiophenes on a non-reduced silver surface has been reported by a SERS study.[11] Adsorption of thiophene and substituted thiophenes on metal surfaces has been investigated using SERS and density functional theory.[12–14] This is because thiophene is similar to pyridine and possesses several adsorption sites such as π electrons of the thiophene ring and the lone pair electrons of the sulfur atom. 3-bromo-2-nitrothiophene as a particularly prominent member of

*For correspondence

Published online: 11 May 2021

the family of substituted thiophenes has attracted attention. The thermodynamic characteristics of adsorption (TCA) of 3-bromo-2-nitrothiophene and other thiophene derivatives have been determined under the conditions of equilibrium gas adsorption chromatography (GAC) on columns with graphitized thermal carbon black (GTCB).[15] The results of the generation and further transformations of the anionic σ-adducts of 3-bromo-2-nitrothiophene and other heteroaromatic systems with selected carbanions in the gas phase have been described.[16] Proton and carbon chemicals shifts and coupling constants have been calculated for 3-bromo-2-nitrothiophene using the density functional theory (DFT) method.[17] Palladium-catalyzed cyanation reactions of 3-bromo-2-nitrothiophene have been investigated.[18]

In this study, we report the SERS study of 3-bromo-2-nitrothiophene which is possessing several sites (sulfur, bromine and oxygen atoms and the π donor thiophene ring) of adsorption. Also, selective enhancement of different vibrational frequency bands of 3-bromo-2-nitrothiophene gives insight into the geometry and orientation of the molecule on the gold surface. The SERS of the 3-bromo-2-nitrothiophene should be recorded only within a potential window between oxidation and reduction potentials to avoid contributions from reduction or oxidation products. Therefore, electrochemical measurements were performed under conditions selected as being particularly suitable for in-situ spectroscopy with surface-enhanced Raman spectroscopy SERS, they served as a basis for the selection of experimental conditions. Additional information obtained from UV–visible spectroscopy as far as was necessary to interpret the SER spectra is included. Also, the adsorption of 3-bromo-2-nitrothiophene is investigated on a gold surface using DFT calculations.

2. Experimental

2.1 *Reagents*

Electrolyte solutions were prepared from acetonitrile (ACN, Merck, >99%) and 0.1 M tetrabutylammonium hexafluorophosphate (TBFP, Fluka). 3-bromo-2-nitrothiophene was synthesized and characterized as described in the supporting information of the previously published work.[19] All solutions were freshly prepared, purged with argon, and all experiments were performed at room temperature (20 °C).

2.2 *Spectroscopic measurements*

In-situ Raman spectra were obtained using a Renishaw 2000 Raman spectrometer employing a charge couple device (CCD) detector with 4 cm^{-1} resolution. SER-spectra were recorded using 647.1 nm exciting laser light. The normal Raman spectrum of the solid 3-bromo-2-nitrothiophene was initially recorded at λ_0 = 647.1 nm (excitation wavelength), however, the obtained spectrum at this wavelength shows a high fluorescence effect and law peak to noise ratio. To decrease the fluorescence effect, the normal Raman spectrum of the solid 3-bromo-2-nitrothiophene was repeated at a lower excitation wavelength (λ_0 = 488 nm). In the recorded normal Raman spectrum of the solid 3-bromo-2-nitrothiophene at λ_0 = 488 nm, the fluorescence effect did not appear. Because of the very low concentration of the 3-bromo-2-nitrothiophene used in the SERS measurements at λ_0 = 647.1 nm, the fluorescence effect was not observed. Infrared spectra were recorded using the Fourier-transform spectrophotometer Shimadzu FT-IR 8400S in the range 4000–400 cm^{-1}.

Roughening of the gold electrode (polycrystalline 99.99%, polished down to 0.3 μ Al_2O_3) employed to confer SERS activity was performed in a separate cell with an aqueous solution of 0.1 **M** KCl by cycling the electrode potential between E_{SCE} = –800 mV and E_{SCE} = 1650 mV for about 15 min.[20] UV-Vis spectra of solutions were recorded with 1.0 cm cuvets on a Shimadzu UV-2101PC spectrometer.

2.3 *Electrochemistry*

Cyclic voltammograms were recorded with a gold disc (6 mm diameter, Bio-Logic Science Instruments SAS) working electrode using 0.1 M TBFP in ACN as supporting electrolyte and SP-50 potentiostat/galvanostat (Bio-Logic Science Instruments SAS) controlled with EC-Lab software package. A silver-silver chloride (Ag/AgCl, Bio-Logic Science Instruments SAS) electrode and a platinum wire (Bio-Logic Science Instruments SAS) were used as reference and counter electrodes, respectively in a one-compartment glass cell (Bio-Logic Science Instruments SAS). All potentials are quoted vs. the silver-silver chloride electrode ($E_{Ag/AgCl}$) except for roughening of the gold electrode the saturated calomel electrode (E_{SCE}) is used.

2.4 *Computational methods*

Calculation of the vibrational spectra of the 3-bromo-2-nitrothiophene was performed using density functional theory DFT (B3LYP) implemented in the software package Gaussian 09.[21] In both approaches a basis set 6-31G (d) was used. The calculated vibrational frequency values obtained as a part of the output from Gaussian 09 software were scaled down uniformly by a factor of 0.9614 as recommended by Scott and Radom.[22] The Gauss-View5.0 by Gaussian Inc. were used for inspecting the input and output files generated by Gaussian09, for preprocessing, structure modification and post-processing analyses of structures, frequencies and forces. To positively identify the most stable structure, the minima, a frequency analysis was performed for each stationary point. These analyses are performed to ensure that all minima have no imaginary frequencies in the vibrational mode calculations. A metallic cluster model was employed to investigate the adsorption of 3-bromo-2-nitrothiophene on the gold surface. The adsorbed 3-bromo-2-nitrothiophene on the gold electrode surfaces was modeled as the metal−molecule complex. The DFT calculations of the metal−molecule complex were carried out with the B3LYP functional. The basis set for C, H, N, O, and S atoms of investigated molecules was 6-31G (d). For the Au atoms, the basis set used was LANL2DZ.

3. Results and Discussion

3.1 *Electrochemistry*

Cyclic voltammogram recorded with a gold electrode in a 0.1M TBFP in ACN with 1 mM 3-bromo-2-nitrothiophene scanned toward positive potentials starting at $E_{Ag/AgCl}$ =0.0 mV shows an anodic wave at $E_{Ag/AgCl}$ = 1889 mV (Figure 1). This anodic wave is associated with a reversible process at $E_{Ag/AgCl}$ = 1077 mV. The half-wave potential for the oxidation of thiophene in different electrolyte solutions was reported in the range of 1.6–2.0 V versus Ag/AgCl reference electrode.[23,24] The andic wave at 1889 mV is attributed to the removal of one electron of the thiophene unit and the formation of 3-bromo-2-nitrothiophene radical cation as an electrochemical oxidation product. This radical cation could proceed to a dimerization process because only one α-position is blocked. The mechanism that describes the formation of radical cation and its proceeding to dimerization process as a result of electrochemical oxidation of five-membered heterocyclic compound are described by Roncali in 1992.[25] Recently, a mechanism was proposed for the electrochemical oxidation of thiophene using low and high oxidation power electrodes.[26] According to this mechanism, the main products for the electrochemical oxidation of thiophene are thiophene-2(5H)-one, 3-hydroxythiophene-2(3H)-one and some other oligomeric thiophene.

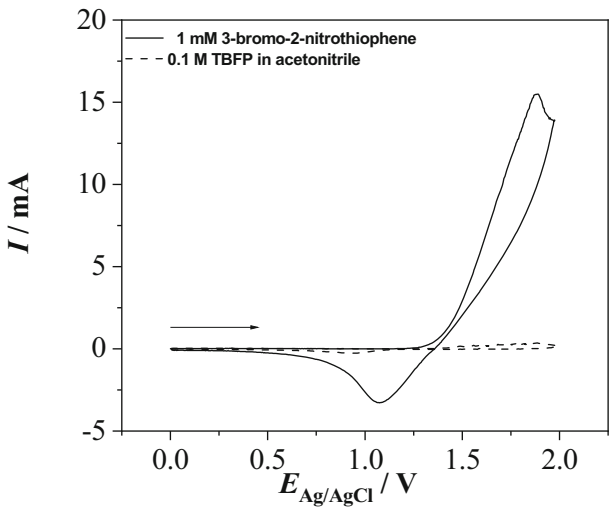

Figure 1. Cyclic voltammograms of a gold disc electrode in a solution of 0.1M TBFP in ACN without/with 1 mM 3-bromo-2-nitrothiophene; (scanning toward positive potentials); dE/dt = 0.15 V s^{-1}, room temperature, argon purged.

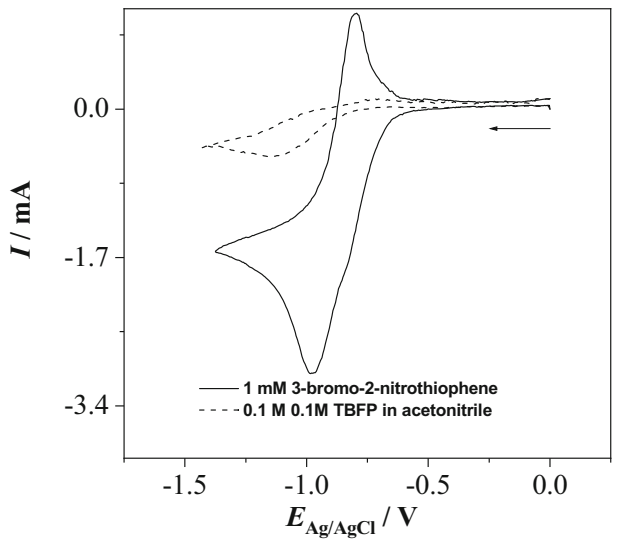

Figure 2. Cyclic voltammograms of a gold disc electrode in a solution of 0.1 M 0.1M TBFP in ACN without/with 1 mM 3-bromo-2-nitrothiophene; (scanning toward negative potentials); dE/dt = 0.15 V s^{-1}, room temperature, argon purged.

In the negative direction scan started at $E_{Ag/AgCl}$ = 0.0 mV the cyclic voltammogram recorded with a gold electrode in a 0.1M TBFP in ACN with 1 mM 3-bromo-2-nitrothiophene shows a cathodic wave at $E_{Ag/AgCl}$ = − 981 mV (Figure 2). This reduction wave is associated with a highly reversible process at $E_{Ag/AgCl}$ = − 768 mV. The reduction process must involve either the nitro or the bromine substituent. Presumably, the reduction involves the nitro group. A reversible cathodic wave was reported at −1050 mV (versus saturated calomel reference electrode) and attributed to the one-electron reduction process of the nitro-group of the nitrothiophene derivatives to form a radical anion.[27,28] In our case, the electrochemical reduction of 3-bromo-2-nitrothiophene to form radical anion could proceed to a dimerization process because only one α-position is blocked.[23] Since the current corresponding to the reversible process at $E_{Ag/AgCl}$ = −768 mV is less than that of the cathodic wave at $E_{Ag/AgCl}$ = −981 mV, the dimerization process is conceivable.

The above electrochemical measurements were performed to determine the suitable potential range for our SERS study. The applied potential in the SERS measurements should be between oxidation and reduction potentials to avoid contributions from reduction or oxidation products.

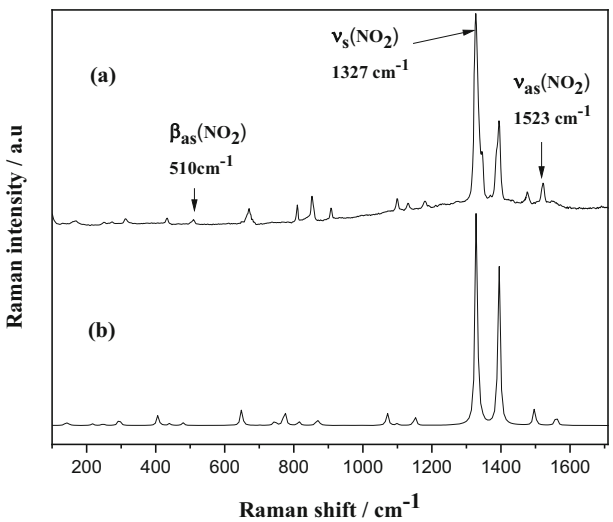

Figure 3. (a) Normal Raman spectrum of the 3-bromo-2-nitrothiophene, resolution 4 cm^{-1}, λ_0 = 488 nm, P_0 = 300 mW and (b) calculated Raman spectrum (normalized, scaled-down uniformly by a factor of 0.9614) of the 3-bromo-2-nitrothiophene according to B3LYP/6-31G (d) level of theory. This figure presents the spectra (a) and (b) as normalized and the spectrum (a) as smoothed.

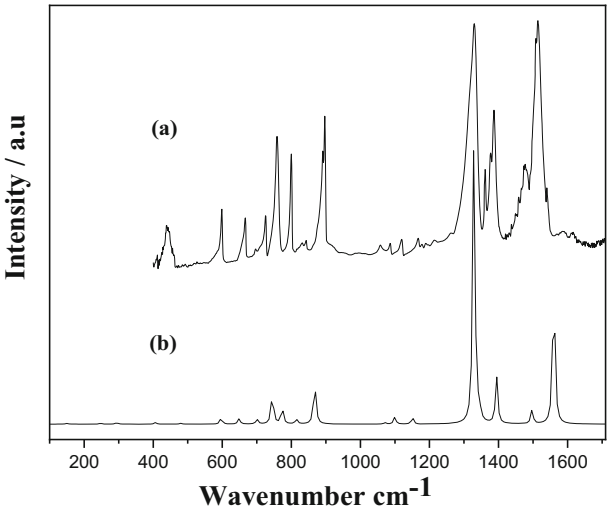

Figure 4. (a) Infrared spectrum of 3-bromo-2-nitrothiophene, resolution 4 cm^{-1}, 32 scans and (b) calculated infrared spectrum of the 3-bromo-2-nitrothiophene according to B3LYP/6-31G (d) level of theory. This figure presents the spectrum (a) as smoothed.

3.2 *Vibrational frequencies of solid 3-bromo-2-nitrothiophene*

The band positions of the calculated and recorded Raman (Figure 3) and infrared (Figure 4) spectra of solid 3-bromo-2-nitrothiophene are listed in Table 1. The profiles of the calculated IR and Raman spectra agree with the observed spectra. Therefore, assignments for the observed IR and Raman bands were made primarily based on the vibrational modes as calculated and on the literature data.[13,14,23,29–31]

3.3 *SER-spectra of adsorbed 3-bromo-2-nitrothiophene on the gold electrode*

To separate conceivable resonance enhancement in Raman spectra from the expected surface enhancement, UV–vis spectrum of the electrolyte solution with added 3-bromo-2-nitrothiophene are recorded. The spectrum, as displayed in Figure 5, shows no relevant absorption close or even in the vicinity of the laser wavelength 647.1 nm employed in SERS. The major band attributed to the π → π* transition is found at 307 nm. Because the excitation wavelength of 647.1 nm used in SERS measurements is far from the UV-vis absorption band, all SERS spectra of adsorbed 3-bromo-2-nitrothiophene were measured under off-resonance conditions.

The SER-spectra of 3-bromo-2-nitrothiophene adsorbed from 0.1 M 0.1M TBFP in ACN electrolyte

Table 1. Assignment of vibrational modes of solid 3-bromo-2-nitrothiophene based on literature data and calculations.

					B3LYP/6-31G (d) Figures 3b and 4b		
Assignment	IR Figure 4a	Raman solid Figure 3a	[a]Vib.#	range[b] (cm^{-1})	Wavenumbers (cm^{-1})	IR absorption	Raman[c] intensity
δ(Skeletal)	–	134	–	–	140	0.184	0.01078
β(C−NO_2)	–	165	–	–	151	0.975	0.00211
γ(ring)	–	–	–	–	216	0.004	0.00511
ν(C−Br)	–	312	–	296–365	294	2.044	0.02367
β(ring)	–	–	–	–	387	2.042	0.0356
γ(ring)	439	433	ν_{21}	414–452	440	0.119	0.00599
$\beta_{as}(NO_2)$	–	510	–	472–557	479	1.161	0.00912
γ(ring)	599	–	ν_{11}	488–644	596	8.449	0.00056
γ(C−H)	668	670	ν_{10}	531–683	649	7.126	0.05975
γ(C−H)	696	–	ν_{19}	531–712	701	6.156	0.0000
β(ring)	726	–	ν_{17}	711–745	745	43.928	0.01778
β(ring)	759	–	ν_{18}	585–763	773	23.465	0.06585
β(C−H)	800	810	ν_{16}	738–918	814	6.393	0.01577
$\beta_s(NO_2)$	833	–	–	830–857	–	–	–
Ring breathing	844	852	ν_3	843–886	867	59.947	0.02532
β(ring)	898	908	ν_8	880–1042	877	0.986	0.00296
β(C−H)	1058	–	ν_7	951–1081	1071	2.042	0.05297
ν_{as}(N−C−S)	1087	1100	–	–	1100	9.651	0.00702
n.a.	1119	1131	–	–	–	–	–
β(C−H)	1178	1180	ν_{15}	1034–1250	1151	9.139	0.04135
$\nu_s(NO_2)$	1330	1327	–	1318–1357	1329	386.101	1.0000
ν(ring)	1361	–	ν_4	1248–1404	1344	17.755	0.01727
ν(ring)	1387	1395	ν_5	1376–1409	1394	63.450	0.74053
ν(ring)	1474	1475	ν_{14}	1459–1507	1497	18.931	0.07946
$\nu_{as}(NO_2)$	1514	1523	–	1487–1555	1559	207.752	0.04998

ν: stretching mode; ν_{as}: asymmetric stretching mode; ν_s: symmetric stretching mode; δ: deformation mode; β: in-plane bending mode; γ: out-of-plane bending mode; β_s: scissoring mode; β_{as}: rocking mode; n.a.: not assigned. [a]: The vibration number and its description according to reference (23). [b]: The range of the vibrational frequencies according to the reported values in literature.[13,14,23,29–31] [c]: normalized intensity.

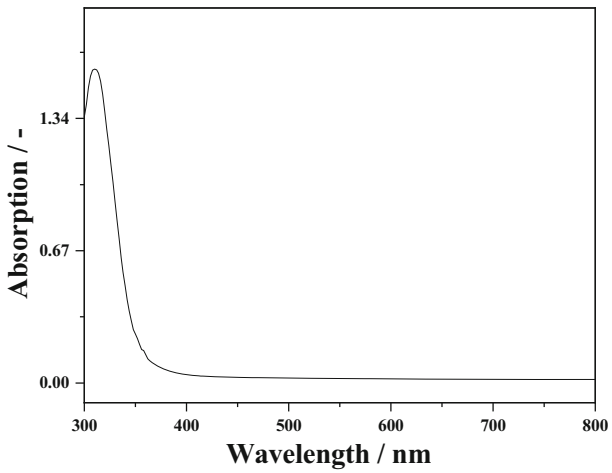

Figure 5. UV–vis spectra of 0.1M TBFP in ACN, with 1mM 3-bromo-2-nitrothiophene, 10 mm cell.

solutions are Figure 6. The assignments of the observed bands of this SER-spectra are listed in Table 2. The SER-spectra of 3-bromo-2-nitrothiophene were initially recorded only within a potential window between oxidation and reduction potentials to avoid contributions from reduction/oxidation products. To determine the interfered SERS bands that correspond to the solvent with those of adsorbed 3-bromo-2-nitrothiophene, the band positions of the SER-spectra of Figure 6 were compared with the reported Raman band positions of the ACN.[32] As a result of this comparison, the bands at 385–389, 925–926, and 1048–1052 cm^{-1} in the SER-spectra of Figure 6 are assigned to the C−C≡N bending (β(C−C≡N)), C−C stretching (*ν*(C−C)) and CH_3 rocking ($\beta_{as}(CH_3)$), respectively, of the adsorbed ACN solvent (Table 2). Also, a comparison between the Raman spectrum of solid 3-bromo-2-nitrothiophene (Figure 3a) and SER-

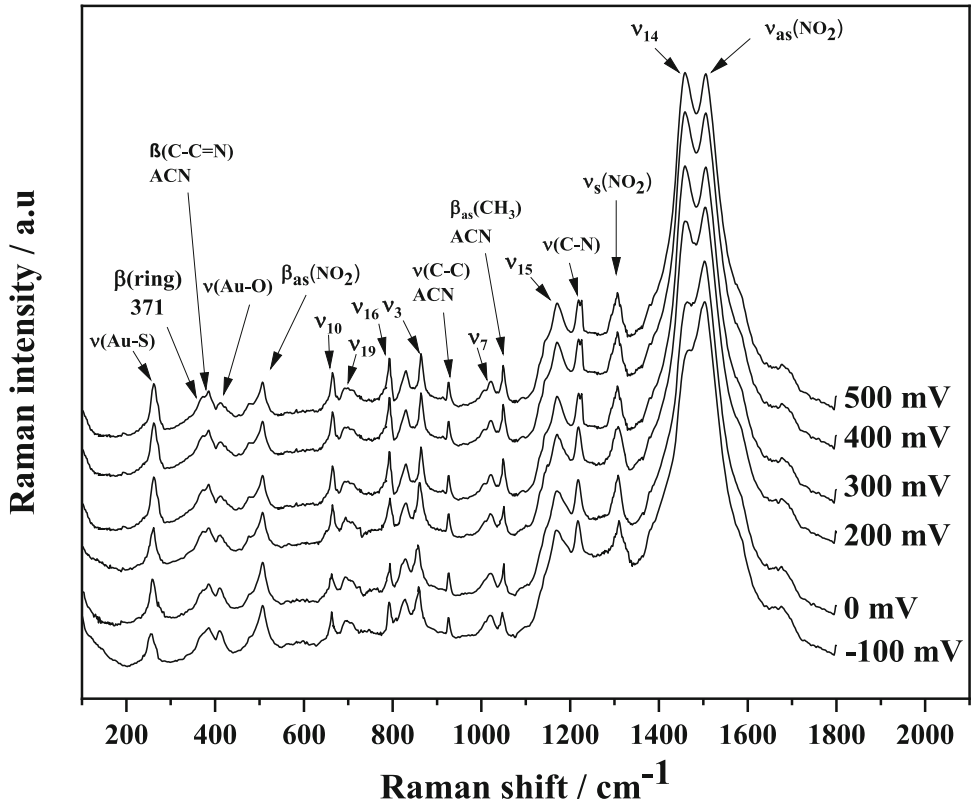

Figure 6. SER- spectra of 1 mM 3-bromo-2-nitrothiophene adsorbed on a gold electrode at electrode potentials as indicated in 0.1M TBFP solution in ACN; λ_0 = 647.1 nm, P_0 100 = mW. This figure presents all spectra as normalized and smoothed. For the vibrations ν_3, ν_7, ν_{10}, ν_{14}, ν_{15}, ν_{16}, and ν_{19} the description according to reference[23].

spectra (Figure 6) shows numerous differences indicative of interactions between the gold surface and the adsorbed molecule. Bands, seen weakly or not at all in the normal Raman spectrum, are observed in SER-spectra of 3-bromo-2-nitrothiophene. The SER-spectra of 3-bromo-2-nitrothiophene show three-band at 256–261, 410–413, and 1216–1219 cm^{-1} (Figure 6). These bands are not observed in Raman and infrared spectra of the solid 3-bromo-2-nitrothiophene. In our case various modes of interaction between adsorbed 3-bromo-2-nitrothiophene and the electrode surface involving the sulfur, bromine, oxygen atoms and the π donor thiophene ring are conceivable. The coordinating capability of the sulfur atom, bromine atom and the oxygen atoms of the nitro-group makes an interaction with the electrode surface *via* these atoms especially likely. In general, the surface-adsorbate vibrational mode can be expected at low wavenumbers. The band at 256–261 cm^{-1} (Figure 6) is assigned to the Au−S stretching mode (*ν*(Au-S), Table 2)). This assignment is based on the reported studies of the adsorbed thiol compounds on gold surfaces by various authors.[33–36] In these studies, Kang *et al*., assigned a band found with cyclohexyl isothiocyanate adsorbed at gold surfaces at 251 and 261 cm^{-1} to the Au-S stretching mode.[34] In the studded self-assembled monolayers of 2-mercaptopyridine on a gold electrode this band was found at 235–243 cm^{-1}.[33] Joo *et al*., found a band at 227 cm^{-1} with benzyl phenyl sulfide adsorbed on a gold sol and assigned it to an Au-S stretching mode.[35] In the study of the adsorption of thiophenol on the gold, the Au-S stretching mode was found at 253–267 cm^{-1}. The second new band at 410–413 cm^{-1} the SER-spectra of 3-bromo-2-nitrothiophene (Figure 6) is assigned to the Au-O stretching mode (ν(Au−O), Table 2). Such a gold–oxygen stretching mode was observed for adsorbed nitroanilines at gold electrodes and it was located at 406–424 cm^{-1}.[37,38] In the normal Raman spectrum of the 3-bromo-2-nitrothiophene (Figure 3a), the NO_2 asymmetric stretching ($\nu_{as}(NO_2)$), NO_2 symmetric stretching ($\nu_s(NO_2)$) and NO_2 rocking ($\beta_{as}(NO_2)$) bands are located at 1523 cm^{-1}, 1327 cm^{-1}, 510 cm^{-1}, respectively (Table 1). These bands are downshifted in the SER-spectra (Figure 6, Table 2) of the 3-bromo-2-nitrothiophene at all applied electrode potentials and are located at 1501−1507 cm^{-1}, 1308−1313 cm^{-1}, 504-507 cm^{-1} for the $\nu_{as}(NO_2)$, $\nu_s(NO_2)$ and $\beta_{as}(NO_2)$ bands, respectively. This downshifting in nitro-group bands and the appearance

Table 2. Assignment of vibrational modes of 3-bromo-2-nitrothiophene adsorbed on a gold electrode at various electrode potentials based on literature data and calculations.[13,14,19–21]

		SERS Figures 6				
Assignment	[a]Vibr.#	$E_{Ag/AgCl}$= −100 mV	$E_{Ag/AgCl}$ = 0 mV	$E_{Ag/AgCl}$ = 200 mV	$E_{Ag/AgCl}$ = 300 mV	$E_{Ag/AgCl}$ = 400 mV
v(Au-S)	–	258	256	257	261	258
γ(ring)[c]	–	371	371	371	371	371
β(C−C≡N)[b]	–	385	385	389	386	385
v(Au-O)	–	410	410	413	411	412
$\beta_{as}(NO_2)$	–	505	504	507	507	506
γ(C−H)	ν_{10}	663	662	662	662	662
γ(C−H)	ν_{19}	697	696	690	699	696
β(C−H)	ν_{16}	792	793	792	792	792
$\beta_s(NO_2)$	–	829	831	831	831	831
Ring breathing	ν_3	858	858	860	864	865
v(C−C)[b]	–	926	926	925	926	925
β(C−H)	ν_7	1021	1021	1019	1022	1023
$\beta_{as}(CH_3)$[b]	–	1049	1048	1052	1051	1052
β(C−H)	ν_{15}	1168	1169	1171	1170	1173
v(C−N)	–	1216	1219	1216	1219	1217
$v_s(NO_2)$	–	1308	1310	1309	1310	1313
v(ring)	ν_{14}	1466	1464	1461	1462	1457
$v_{as}(NO_2)$	–	1503	1501	1505	1507	1505

v: stretching mode; v_{as}: asymmetric stretching mode; v_s: symmetric stretching mode; β: in-plane bending mode; γ: out-of-plane bending mode; β_s: scissoring mode; β_{as}: rocking mode. [a]: The Vibration number and its description according to reference (23). [b]: Bands correspond to the adsorbed ACN solvent and are assigned according to the reference (32). [c]: band appeared as a shoulder at −100, 0, 200, and 300 mV electrode potentials and as a separated band at electrode potentials higher than 300 mV.

of the Au-O stretching mode support the assumed adsorption *via* the nitro group. Further supports for the interaction of the nitro group of the adsorbed 3-bromo-2-nitrothiophene with the gold surface the appearance of the third new band at 1216−1219 cm^{-1} (Figure 6). This band was assigned to the C−N stretching mode (ν(C−N), Table 2).[29] Adsorption of the 3-bromo-2-nitrothiophene *via* bromine atom with the gold surface is excluded. The C−Br stretching mode is absent in the SER-spectra of the adsorbed 3-bromo-2-nitrothiophene at gold.

The orientation of the adsorbed molecule with respect to the electrode surface can be deduced from the shift, appearance and disappearance of bands in surface spectra compared with normal spectra. In the SER spectra of the adsorbed 3-bromo-2-nitrothiophene several bands correspond to the ring breathing (ν_3), in-plane C−H bending (ν_{16}, ν_7, ν_{15}) and ring stretching (ν_{14}) modes were observed (Table 2, Figure 6). The appearance of these modes suggests a vertical orientation of the thiophene ring of 3-bromo-2-nitrothiophene with respect to the gold surface. In contrast, two modes observed at 690–697 cm^{-1} (ν_{19}) and 662–663 cm^{-1} (ν_{10}) caused by C−H out of plane bending modes (γ(C-H)) of the thiophene ring vibration in the SER spectra supports a flat orientation the thiophene ring with respect to the gold surface. According to the surface selection rule reported by Moskovits and co-workers,[39–42] the relative intensity of the thiophene ring modes in the SERS spectrum provides a key to the surface orientation of adsorbed molecules. The ring breathing (ν_3), ring stretching (ν_{14}) and in-plane C−H bending (ν_{16}, ν_7, ν_{15}) modes are expected to be weak for flat-oriented thiophene ring of 3-bromo-2-nitrothiophene, whereas for an orientation with the thiophene ring vertical it should be fairly strong. In the present case, the intensities of these bands (ν_3, ν_{14}, ν_{16}, ν_7, ν_{15}) are medium to strong (Figure 6). This implies a vertical or at least tilted orientation of the adsorbed molecules with respect to the gold surface. Further supports to this result, is the weak and broad appearance of the out-of-plane C−H bending modes (ν_{19} at 690–697 cm^{-1}, ν_{10} at 662–663 cm^{-1}) of the thiophene ring in the SER-spectra of 3-bromo-2-nitrothiophene (Figure 6). Remarkable potential-dependent changes in intensity can be observed for the ring stretching

(ν_{14}, at 1457−1466 cm^{-1}) and $\nu_{as}(NO_2)$ modes (Figure 6). As the electrode potential increased in the direction of positive potential the intensity of the ring stretching mode (ν_{14}) mode is increased, while the intensity of the $\nu_{as}(NO_2)$ mode is almost not changed. This implies a less tilted or even vertical orientation of the adsorbed 3-bromo-2-nitrothiophene at more positive electrode potentials. Another noteworthy aspect of the SER spectra of Figure 6 is at the electrode potentials −100, 0, 200 and 300 mV a shoulder band appeared at 371 cm^{-1}. This band was nearly separated from the band that corresponds to ACN ($\beta(C-C\equiv N)$) solvent at higher electrode potentials (400 mV and 500 mV). Also, this band was very close to the in-plane bending of the thiophene ring (β(ring)) that appeared at 387 cm^{-1} in the calculated Raman spectrum 3-bromo-2-nitrothiophene, while, do not has a counterpart in the recorded normal Raman spectrum 3-bromo-2-nitrothiophene and the reported Raman spectrum of the ACN solvent.[32] Therefore, it was assigned to the in-plane bending of the thiophene ring (β(ring)). The appearance of the band located at 371 cm^{-1} (Figure 6) as a separated band, supports a less tilted orientation of the adsorbed 3-bromo-2-nitrothiophene at more positive electrode potentials. It should be mentioned that the Raman intensities are considerably decreased at the 500 mV electrode potential. Because all SER-spectra is normalized, the decrease in Raman intensities at this electrode potential (500 mV) is not clear in Figure 6. The decrease in Raman intensities can be attributed to the change in orientation of the adsorbed 3-bromo-2-nitrothiophene at higher electrode potential (500 mV) as discussed above.

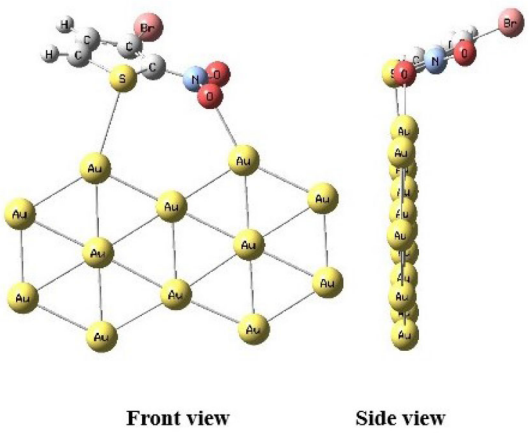

Figure 7. Optimized structure of the adsorbed 3-bromo-2-nitrothiophene on Au surface according to DFT calculation.

3.4 *DFT calculations of the adsorbed 3-bromo-2-nitrothiophene on Au surface*

According to the DFT calculation, the optimized structure of the adsorbed 3-bromo-2-nitrothiophene on Au surface is displayed in Figure 7. As shown in this figure, a tilted adsorption orientation was found of the 3-bromo-2-nitrothiophene on the Au surface.

Figure 8 presents the simulated Raman spectrum of 3-bromo-2-nitrothiophene on a gold surface. The Raman spectrum of 3-bromo-2-nitrothiophene on the gold surface is dominated by several strong to medium bands at 806, 830, 857, 1039, 1141, 1226, 1310, 1488, and 1539 cm^{-1}. The bands at 806, 1039, and 1141 cm^{-1} are assigned to the in-plane C−H bending modes (β(C−H)) ν_{16}, ν_7, and ν_{15}, respectively. The bands at 830, 857, 1226, 1310, 1488, and 1539 cm^{-1} are assigned to the NO_2 scissoring ($\beta_s(NO_2)$), thiophene ring breathing (ν_3), C−N stretching (ν(C−N)), NO_2 symmetric stretching ($\nu_s(NO_2)$), thiophene ring stretching (ν_{14}) and NO_2 asymmetric stretching ($\nu_{as}(NO_2)$) modes, respectively. The appearance of the ν_{16}, ν_7, ν_{15}, ν_{14}, ν_3, $\beta_s(NO_2)$, ν(C−N), $\nu_s(NO_2)$ and $\nu_{as}(NO_2)$ bands as strong to medium bands agree with the tilted orientation of the adsorbed 3-bromo-2-nitrothiophene molecule with respect to the gold surface as displayed in Figure 7. Further supports for this result is the appearance of the weak out-of-plane bending modes at 681 (ν_{19}, γ(C−H)), 642 (ν_{10}, γ(C−H)), 590 (ν_{11}, γ(ring)) and 181 (γ(ring)) cm^{-1} (Figure 8). The adsorption 3-bromo-2-nitrothiophene on the gold surface via the nitro group and the sulfur atom described in Figure 7, can be indicated from the appearance of the Au-O stretching (ν(Au−O)) and Au-S stretching (ν(Au−S)) modes at 426 and 275 cm^{-1}, respectively, in the Calculated SER-spectrum of the 3-bromo-2-nitrothiophene (Figure 8). It should be noted that the ν(Au−O), ν(Au−S), and ν(C−N) bands of Figure 8 have not appeared in the calculated Raman spectrum of the free 3-bromo-2-nitrothiophene molecule (Table 1, Figure 3). Additional very weak modes appear in the calculated SER-spectrum of the adsorbed 3-bromo-2-nitrothiophene on Au surface (Figure 8) at 1420, 474, 379, 157, and 134 cm^{-1} and are assigned to ring stretching (ν_5, ν(ring)), NO_2 rocking ($\beta_{as}(NO_2)$), in-plan ring bending (β(ring)), in-plane C−NO_2 bending (β(C−NO_2)) and skeletal deformation (δ(skeletal)) modes, respectively. The perfect matching between the calculated SER-spectrum of the adsorbed 3-bromo-2-nitrothiophene (Figure 8) with those recorded (Figure 6) makes us believe that the 3-bromo-2-nitrothiophene adsorbed on the Au surface

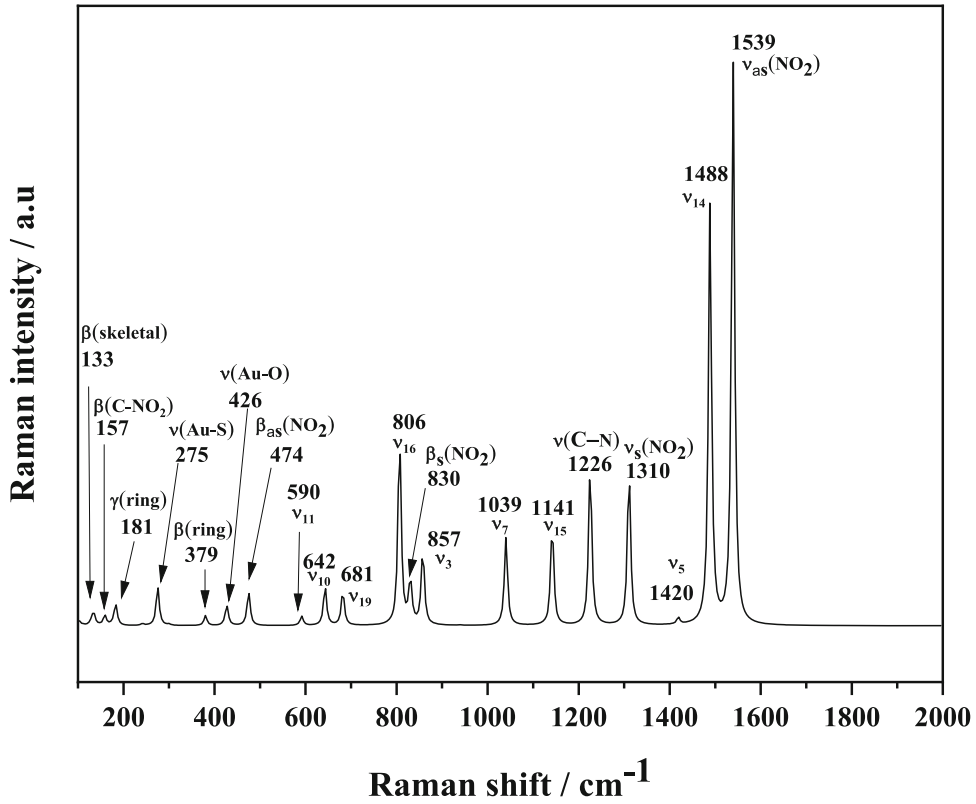

Figure 8. Calculated SER-spectrum of the adsorbed 3-bromo-2-nitrothiophene on Au surface. This figure presents the spectrum as normalized. For the vibrations ν_3, ν_5, ν_7, ν_{10}, ν_{11}, ν_{14}, ν_{15}, ν_{16}, and ν_{19} the description according to reference (23).

in a tilted orientation and *via* the nitro group and the sulfur atom (Figure 7).

4. Conclusions

3-bromo-2-nitrothiophene adsorbs strongly on the polycrystalline gold surface *via* sulfur and oxygen atoms of the nitro group that interacting directly with the gold surface. This is evidenced by the appearance of low-wavenumber bands in the SER-spectra of the 3-bromo-2-nitrothiophene, which corresponds to gold-oxygen and gold-sulfur stretching frequencies. Numerous bands in the SER-spectra of the 3-bromo-2-nitrothiophene showing slight shifts when compared to the free molecule are found. In-plane modes dominate in the SER-spectra of the 3-bromo-2-nitrothiophene implying a perpendicular position of the adsorbate. The results of the calculated SER-spectrum are in perfect agreement with those obtained experimentally. The electrochemical oxidation and reduction of the 3-bromo-2-nitrothiophene were determined at the gold electrode. Reversible anodic and cathodic waves were observed in the cyclic voltammograms of the 3-bromo-2-nitrothiophene.

References

1. Bae S J, Lee C R, Choi I S, Hwang C S, Gong M S, Kim K and Joo S W 2002 Adsorption of 4-biphenylisocyanide on gold and silver nanoparticle surfaces: surface-enhanced raman scattering study *J. Phys. Chem. B* **106** 7076
2. Pagliai M, Caporali S, Muniz-Miranda M, Pratesi G and Schettino V 2012 SERS, XPS, and DFT study of adenine adsorption on silver and gold surfaces *J. Phys. Chem. Lett.* **3** 242
3. Kudelski A 2003 Chemisorption of 2-mercaptoethanol on silver, copper, and gold: direct raman evidence of acid-induced changes in adsorption/desorption equilibria *Langmuir* **19** 3805
4. Bloxham S, Eicher-Lorka O, Jakubėnas R and Niaura G 2003 Adsorption of cysteamine at copper electrodes as studied by surface-enhanced raman spectroscopy *Spectrosc. Lett.* **36** 211
5. Królikowska A, Kudelski A, Michota A and Bukowska J 2003 SERS studies on the structure of thioglycolic acid monolayers on silver and gold *Surf. Sci.* **532–535** 227
6. Kania S and Holze R 1998 Surface enhanced Raman spectroscopy of anions adsorbed on foreign metal modified gold electrodes *Surf. Sci.* **408** 252
7. Costa J C S, Ando R A, Camargo P H C and Corio P 2011 Understanding the effect of adsorption geometry over substrate selectivity in the surface-enhanced raman

scattering spectra of simazine and atrazine *J. Phys. Chem. C* **115** 4184
8. Takahashi M, Fujita M and Ito M 1984 Surface-enhanced Raman spectra and molecular orientation of phthalazine adsorbed on a silver electrode *Chem. Phys. Lett.* **109** 122
9. Irish D E, Guzonas D and Atkinson G F 1985 Surface enhanced Raman spectroscopy of the silver/KCl, triethylenediamine (DABCO), water system *Surf. Sci.* **158** 314
10. Netzer F P and Ramsey M G 1992 Structure and orientation of organic molecules on metal surfaces *Crit. Rev.* **17** 397
11. Bukowska J 1992 Surface-enhanced Raman scattering spectra as a probe of adsorbate-surface interaction *J. Mol. Struct.* **275** 151
12. Majumder C, Mizuseki H and Kawazoe Y 2003 Thiophene thiol on the Au(111) surface: size-dependent adsorption study *J. Chem. Phys.* **118** 9809
13. Mukherjee K, Bhattacharjee D and Misra T N 1999 Surface enhanced raman spectroscopic study of isomeric methylthiophenes in silver colloid *J. Colloid Interface Sci.* **213** 46
14. Mukherjee K M and Misra T N 1997 Surface enhanced Raman spectroscopic study of 2- and 3-chloro-thiophene in silver hydrosol *Spectrochim. Acta A* **53** 1439
15. Yashkin S N, Yashkina E A, Svetlov D A and Murashov B A 2019 Adsorption and chromatographic separation of thiophene derivatives on graphitized thermal carbon black russ *J. Phys. Chem. A* **93** 2482
16. Zimnicka M and Danikiewicz W 2015 Gas-phase anionic σ-adduct (trans)formations in heteroaromatic systems *J. Am. Soc. Mass Spectrom.* **26** 1191
17. Katritzky A R, Akhmedov N G, Doskocz J, Hall C D, Akhmedova R G and Majumder S 2007 Structural elucidation of nitro-substituted five-membered aromatic heterocycles utilizing GIAO DFT calculations *Magn. Reson. Chem.* **45** 5
18. Erker T and Nemec S 2004 Palladium-Catalyzed Cyanation Reactions of Thiophene Halides *Synthesis* **1** 23
19. Sartori L, Mercurio C, Amigoni F, Cappa A, Fagá G, Fattori R, Legnaghi E, Ciossani G, Mattevi A, Meroni G, Moretti L, Cecatiello V, Pasqualato S, Romussi A, Thaler F, Trifiró P, Villa M, Vultaggio S, Botrugno O A, Dessanti P, Minucci S, Zagarrí E, Carettoni D, Iuzzolino L, Varasi M and Vianello P 2017 Thieno[3,2-b]pyrrole-5-carboxamides as new reversible inhibitors of histone lysine demethylase KDM1A/LSD1. Part 1: high-throughput screening and preliminary exploration *J. Med. Chem.* **60** 1673
20. Holze R 1988 Preparation of gold electrodes for surface enhanced Raman spectroscopy SERS *Surf. Sci.* **202** L612
21. Gaussian 09, Revision A.01, Frisch M J, Trucks G W, Schlegel H B, Scuseria G E, Robb, M A Cheeseman, J R; Scalmani G Barone, V Mennucci, B Petersson G A; Nakatsuji H Caricato M, Li X, Hratchian, H P Izmaylov, A F.; Bloino, J Zheng, G Sonnenberg, J L Hada, M Ehara, M Toyota, K Fukuda, R Hasegawa, J Ishida, M Nakajima, T Honda, Y Kitao, O Nakai, H Vreven, T Montgomery, J A Jr., Peralta, J E Ogliaro, F Bearpark, M. Heyd, J J Brothers, E Kudin, K, J W; Martin, R L Morokuma, K Zakrzewski, V G Voth, G A Salvador, P Dannenberg, J J.; Dapprich, S Daniels, A D; Farkas, Ö Foresman, J B Ortiz, J V Cioslowski, J and Fox, D J Nakatsuji, H Caricato, M. Li, X. Hratchian, H P Izmaylov, A F Bloino, J Zheng, G Sonnenberg, J L Hada, M Ehara, M Toyota, K Fukuda, R Hasegawa, J Ishida, M Nakajima, T Honda, Y Kitao, O Nakai, H Vreven, T Montgomery, J A Jr., Peralta, J E Ogliaro, F Bearpark, Heyd, M J J Brothers, E Kudin, K N Staroverov, V N Kobayashi, R Normand, J Raghavachari, K Rendell, A Burant, J C Iyengar, S S Tomasi, J Cossi, M Rega, N Millam, J M Klene, M J Knox, E Cross, J B Bakken, V Adamo, C Jaramillo, J Gomperts, R Stratmann, R E Yazyev, O Austin, A J Cammi, R Pomelli, C Ochterski, J W Martin, R L Morokuma, K Zakrzewski, V G Voth, G A Salvador, P Dannenberg, J J Dapprich, S Daniels, A D Farkas, Ö Foresman, J B Ortiz, J V Cioslowski, J and Fox D J. Gaussian, Inc., Wallingford CT, 2009.
22. Scott A P and Radom L 1996 Harmonic vibrational frequencies: an evaluation of hartree−fock, møller−plesset, quadratic configuration interaction, density functional theory, and semiempirical scale factors *J. Phys. Chem.* **100** 16502
23. Gronowitz S 1991 *Chemistry of Heterocyclic Compounds: Thiophene and Its Derivatives* Part Four, Vol. 44 (US: John Wiley & Sons)
24. Kuwabata S, Ito S and Yoneyama H 1988 Copolymerization of pyrrole and thiophene by electrochemical oxidation and electrochemical behavior of the resulting copolymers *J. Electrochem. Soc.* **135** 1691
25. Roncali J 1992 Conjugated poly(thiophenes): synthesis, functionalization, and applications *Chem. Rev.* **92** 711
26. Mehri F, Sauter W, Schröeder U and Rowshanzamir S 2019 Possibilities and constraints of the electrochemical treatment of thiophene on low and high oxidation power electrodes *Energy Fuels* **33** 1901
27. Breccia A, Busi F, Gattavecchia E and Tamba M 1990 Reactivity of nitro-thiophene derivatives with electron and oxygen radicals studied by pulse radiolysis and polarographic techniques *Radiat. Environ. Biophys.* **29** 153
28. Boga C, Calvaresi M, Franchi P, Lucarini M, Fazzini S, Spinelli D and Tonelli D 2012 Electron reduction processes of nitrothiophenes. A systematic approach by DFT computations, cyclic voltammetry and E-ESR spectroscopy *Org. Biomol. Chem.* **10** 7986
29. Lin-Vien D, Colthup N B, Fateley W G and Grasselli J G 1991 *The Handbook of Infrared and Raman Characteristic Frequencies of Organic Molecules* (Academic Press: San Diego)
30. Mukherjee K M and Misra T N 1997 Surface enhanced raman spectroscopic study of 2- and 3-bromothiophenes in silver hydrosol *Bull. Chem. Soc. Jpn.* **70** 301
31. Bazzaoui E A, Bazzaoui M, Aubard J, Lomas J S, Félidj N and Lévi G 2001 Surface-enhanced Raman scattering study of polyalkylthiophenes on gold electrodes and in silver colloids *Synth. Met.* **123** 299
32. Neelakantan P 1964 Raman spectrum of acetonitrile *Proc. Indian Acad. Sci. – Sec. A* **60** 422

33. Hassan N and Holze R 2012 Surface enhanced Raman spectroscopy of self-assembled monolayers of 2-mercaptopyridine on a gold electrode *Russ. J. Electrochem.* **48** 401
34. Kang H, Noh J, Ganbold E-O, Uuriintuya D, Gong M-S, Oh J J, et al. 2009 Adsorption changes of cyclohexyl isothiocyanate on gold surfaces *J. Colloid Interface Sci.* **336** 648
35. Joo S W, Han S W and Kim K 2000 Surface-enhanced raman scattering of aromatic sulfides in aqueous gold sol *Appl. Spectrosc.* **54** 378
36. Holze R 2015 The adsorption of thiophenol on gold – a spectroelectrochemical study *Phys. Chem. Chem. Phys.* **17** 21364
37. Holze R 1990 The adsorption of p-nitroaniline on silver and gold electrodes as studied with surface enhanced Raman spectroscopy (SERS) *Electrochim. Acta* **35** 1037
38. Jbarah AA and Holze R 2006 A comparative spectroelectrochemical study of the redox electrochemistry of nitroanilines *J. Solid State Electr.* **10** 360
39. Moskovits M 1982 Surface selection rules *J. Chem. Phys.* **77** 4408
40. Moskovits M and Suh J S 1984 The geometry of several molecular ions adsorbed on the surface of colloidal silver *J. Phys. Chem.* **88** 1293
41. Moskovits M and Suh J S 1984 Surface selection rules for surface-enhanced Raman spectroscopy: calculations and application to the surface-enhanced Raman spectrum of phthalazine on silver *J. Phys. Chem.* **88** 5526
42. Moskovits M, DiLella D P and Maynard K J 1988 Surface Raman spectroscopy of a number of cyclic aromatic molecules adsorbed on silver: selection rules and molecular reorientation *Langmuir* **4** 67